



**HAL**  
open science

# Torque optimization of seven phase BLDC machines in normal and degraded modes with constraints on current and voltage

Duc Tan Vu, Ngac Ky Nguyen, Eric Semail, Tiago José dos Santos Moraes

## ► To cite this version:

Duc Tan Vu, Ngac Ky Nguyen, Eric Semail, Tiago José dos Santos Moraes. Torque optimization of seven phase BLDC machines in normal and degraded modes with constraints on current and voltage. PEMD 2018, the 9th International Conference on Power Electronics, Machines and Drives, Apr 2018, Liverpool, United Kingdom. hal-01882858

**HAL Id: hal-01882858**

**<https://hal.science/hal-01882858v1>**

Submitted on 27 Sep 2018

**HAL** is a multi-disciplinary open access archive for the deposit and dissemination of scientific research documents, whether they are published or not. The documents may come from teaching and research institutions in France or abroad, or from public or private research centers.

L'archive ouverte pluridisciplinaire **HAL**, est destinée au dépôt et à la diffusion de documents scientifiques de niveau recherche, publiés ou non, émanant des établissements d'enseignement et de recherche français ou étrangers, des laboratoires publics ou privés.

# Torque optimization of seven-phase BLDC machines in normal and degraded modes with constraints on current and voltage

*Duc Tan Vu, Ngac Ky Nguyen, Eric Semail, Tiago Jose dos Santos Moraes*

*Univ. Lille, Centrale Lille, Arts et Metiers ParisTech, HEI, EA 2697 - L2EP - Laboratoire d'Electrotechnique et d'Electronique de Puissance, F-59000 Lille, France.*

*E-mail: {ductan.vu; ngacky.nguyen; eric.semail; tiago.dossantosmoraes}@ensam.eu*

**Keywords:** seven-phase BLDC machine; torque optimization; current and voltage limits; fault-tolerant control; analytical formulation.

## Abstract

This paper proposes several easy-to-implement control strategies when seven-phase axial flux brushless DC machines with trapezoidal back electromotive forces operate in normal and faulty modes by taking into account constraints on voltage and current. The constraints are related to the converter and machine design in terms of maximum values of current and voltage. The considered faults are cases in which one or two phases of the machine are open-circuited. Numerical computations based on analytical formulations are applied to obtain torque-speed characteristics, including the flux-weakening operation. The methods determine current references to ensure the torque optimizations while currents and voltages are within their limits. The usefulness of the methods is verified by numerical results.

## 1 Introduction

Variable-speed electric drives using multiphase machines have been known for a half of century. The interest in this area has been growing significantly during the last decade because of developments in some specific uses. The design, modeling and control methods in healthy and faulty modes are summarized and analyzed in [1, 2]. Better fault-tolerance from faults of the power converters is a main advantage of multiphase machines compared with conventional three-phase machines. Many strategies have been proposed to maximize torque with a certain copper loss ratio by determining appropriate current references when one or more phases of the machines are open-circuited.

In [3], fault-tolerant control strategies for seven-phase machines using a vectoral multiphase description are verified with single and double open-circuit faults. However, these approaches have not considered constraints on current and voltage which play an important role in the sizing and cost of VSI. In addition, for wide speed-range applications such as electric vehicles, it is necessary to take into account flux-weakening strategies in the systems to guarantee machine-converter voltage limits. In [4-6], the fundamental and third-harmonic current components for the excitation in healthy

stator phases are introduced for five-phase permanent-magnet motors with trapezoidal back-EMFs in open-phase faults but the flux-weakening operation has not been considered. In these studies, there are eight unknown variables in current expressions determined by Fmincon in MATLAB. By the same way, the seven-phase machines need more variables, which makes current reference calculations more complicated and less accurate due to sensitivity of Fmincon on the number of variables. In [7], an interesting approach is proposed for 5-phase fault-tolerant PM machines by defining a weighting factor to adjust the degree of flux-weakening, which either optimizes copper losses in healthy operation or limits phase currents in case of open-circuit and short-circuit faults. Nonetheless, currents obtained by this approach contain high frequency components which limit the range of speed. A variable speed control method in [8] considering voltage and current limits is applied to a 5-phase permanent magnet synchronous generator with sinusoidal back-EMFs under healthy and faulty conditions, including flux-weakening operation. Authors in [9] have proposed different control strategies for odd and even phase sinusoidal machines in one opened-phase fault without considering maximum currents and voltages as well as the flux-weakening operation. New current references for the degraded mode ensure the same rotating magnetic field as in healthy mode. The strategies in [8, 9] are only introduced for sinusoidal back-EMF machines.

Several studies based on reduced-order Park and Concordia transformation matrices with the aim of preserving values of magnetomotive forces (MMFs) under single and double phase open faults have been introduced in recent years. A method in [10] only deals with sinusoidal back-EMF machines while the first and third harmonics of back-EMFs are considered in [11], but only sinusoidal current references are imposed in those two papers, leading to uneliminated torque ripples. In [12], both the first and the third harmonic current references are injected to trapezoidal back-EMF machines to generate free-ripple torques. Nevertheless, the strategies in [10-12] do not take into account constraints on voltage as well as the flux-weakening operation.

In this paper, control strategies for healthy and faulty cases are proposed to optimize the torque of a seven-phase axial flux brushless DC machine with double identical rotors under constraints on current and voltage. The first and third harmonics of back EMFs are considered; therefore, the first and third harmonic currents are imposed to generate torque.

$$T = \sqrt{\frac{2}{7}} \begin{bmatrix} \frac{1}{\sqrt{2}} & \frac{1}{\sqrt{2}} & \frac{1}{\sqrt{2}} & \frac{1}{\sqrt{2}} & \frac{1}{\sqrt{2}} & \frac{1}{\sqrt{2}} & \frac{1}{\sqrt{2}} \\ \cos\theta & \cos\left(\theta - \frac{2\pi}{7}\right) & \cos\left(\theta - \frac{4\pi}{7}\right) & \cos\left(\theta - \frac{6\pi}{7}\right) & \cos\left(\theta - \frac{8\pi}{7}\right) & \cos\left(\theta - \frac{10\pi}{7}\right) & \cos\left(\theta - \frac{12\pi}{7}\right) \\ -\sin\theta & -\sin\left(\theta - \frac{2\pi}{7}\right) & -\sin\left(\theta - \frac{4\pi}{7}\right) & -\sin\left(\theta - \frac{6\pi}{7}\right) & -\sin\left(\theta - \frac{8\pi}{7}\right) & -\sin\left(\theta - \frac{10\pi}{7}\right) & -\sin\left(\theta - \frac{12\pi}{7}\right) \\ \cos 5\theta & \cos\left(5\theta - \frac{4\pi}{7}\right) & \cos\left(5\theta - \frac{8\pi}{7}\right) & \cos\left(5\theta - \frac{12\pi}{7}\right) & \cos\left(5\theta - \frac{16\pi}{7}\right) & \cos\left(5\theta - \frac{20\pi}{7}\right) & \cos\left(5\theta - \frac{24\pi}{7}\right) \\ -\sin 5\theta & -\sin\left(5\theta - \frac{4\pi}{7}\right) & -\sin\left(5\theta - \frac{8\pi}{7}\right) & -\sin\left(5\theta - \frac{12\pi}{7}\right) & -\sin\left(5\theta - \frac{16\pi}{7}\right) & -\sin\left(5\theta - \frac{20\pi}{7}\right) & -\sin\left(5\theta - \frac{24\pi}{7}\right) \\ \cos 3\theta & \cos\left(3\theta - \frac{6\pi}{7}\right) & \cos\left(3\theta - \frac{12\pi}{7}\right) & \cos\left(3\theta - \frac{18\pi}{7}\right) & \cos\left(3\theta - \frac{24\pi}{7}\right) & \cos\left(3\theta - \frac{30\pi}{7}\right) & \cos\left(3\theta - \frac{36\pi}{7}\right) \\ -\sin 3\theta & -\sin\left(3\theta - \frac{6\pi}{7}\right) & -\sin\left(3\theta - \frac{12\pi}{7}\right) & -\sin\left(3\theta - \frac{18\pi}{7}\right) & -\sin\left(3\theta - \frac{24\pi}{7}\right) & -\sin\left(3\theta - \frac{30\pi}{7}\right) & -\sin\left(3\theta - \frac{36\pi}{7}\right) \end{bmatrix} \quad (6)$$

In case of one opened-phase fault, four different methods are introduced. When two phases are open-circuited, optimal torques are obtained by determining the first and third harmonics of current references in d-q frames.

The paper is organized as follows: Section 2 describes the modeling of the considered machine. The control strategies for different operating conditions are demonstrated in Section 3 and Section 4 gives numerical results.

## 2 Multi-phase Machine Modeling

The design of a seven-phase BLDC machine is proposed in [13, 14] with axial flux and double identical rotors. These following assumptions are considered to model the machine: 7 phases of the machine are equally shifted and wye-connected; the machine has trapezoidal back-EMFs; the saturation of the magnet circuits is not considered in the calculation of the back-EMFs and the fluxes. The voltage vector and torque can be written as follows:

$$\vec{v} = R\vec{i} + \Lambda \frac{d\vec{i}}{dt} + \vec{e} \quad (1)$$

$$T_m = \frac{\vec{e} \cdot \vec{i}}{\Omega} \quad (2)$$

where  $\vec{v}$ ,  $\vec{i}$  and  $\vec{e}$  are 7-dimensional stator voltage, current and back-EMF vectors, respectively;  $R$  is the stator resistance of each phase;  $\Lambda$  is a 7 by 7 stator inductance matrix;  $T_m$  is the torque and  $\Omega$  is the rotating speed of the machine.

Concordia and Park transformations are applied to convert the machine into  $\alpha$ - $\beta$  and d-q frames. In these frames, the seven-phase machine is equivalent to 3 fictitious 2-phase machines (FM1, FM2 and FM3) and 1 zero-sequence machine [15, 16]. The harmonic characterization of the fictitious machines is described in [14]. FM1 is the main machine associated to the first harmonics and FM2 is the secondary machine representing the fifth harmonics. FM3 is the third machine with the third harmonics. Since the machine is wye-connected; therefore, the zero-sequence machine is not considered.

## 3 Control methods with constraints on current and voltage

### 3.1 Healthy mode

The machine under this study has trapezoidal back-EMFs. Besides the first harmonics, only the third harmonics of the back-EMFs are considered since their amplitude equals to about 19% of the fundamental harmonics while that of other higher harmonics is tiny (0.4%, 6.9%, and 6.2% for the fifth,

seventh and ninth harmonics, respectively) [3]. Basically, there is no torque ripple in healthy mode, but a fault leads to torque ripples due to these high harmonics of the back-EMFs. However, since their magnitudes are very low, the created torque ripples are not considered. In healthy mode, using the first and third harmonics of currents gives optimal torque-speed characteristics with respect to the constraints on current and voltage. These currents are obtained by solving Equation (3).

$$\vec{i} = (T^{-1})\vec{i}_{dq} \quad (3)$$

where  $T$  is the transformation matrix in Equation (6);  $\theta$  is the electrical angle;  $\vec{i} = [i_a \ i_b \ i_c \ i_d \ i_e \ i_f \ i_g]^T$  is a current vector in natural frame;  $\vec{i}_{dq} = [0 \ i_{d1} \ i_{q1} \ i_{d5} \ i_{q5} \ i_{d3} \ i_{q3}]^T$  is a current vector in the rotating d-q frames.

In healthy mode, as the system is balanced, equations for only one phase needs to be written. Constraints on current and voltage in phase a can be expressed in Equations (4-5).

$$|i_a| = \sqrt{\frac{2}{7}} |i_{d1} \cos\theta - i_{q1} \sin\theta + i_{d3} \cos 3\theta - i_{q3} \sin 3\theta| \leq I_{max} \quad (4)$$

$$|v_a| = \left| R i_a + L \frac{di_a}{dt} + M1 \left( \frac{di_b}{dt} + \frac{di_g}{dt} \right) + M2 \left( \frac{di_c}{dt} + \frac{di_f}{dt} \right) + M3 \left( \frac{di_d}{dt} + \frac{di_e}{dt} \right) + e_a \right| \leq V_{max} \quad (5)$$

where  $I_{max}$  and  $V_{max}$  are current and voltage limits according to the converter and machine parameters.

Conventionally,  $V_{max}$  is equal to a half of the DC bus voltage in the Pulse Width Modulation technique.  $I_{max}$  is based on the instantaneous peak currents during a short-time operation and it is related to VSI components. In addition,  $I_{max}$  is also based on the maximum thermal currents depending on windings temperature.  $M_1$ ,  $M_2$ , and  $M_3$  are mutual inductances between phase a and other phases of the machine. The strategy aims at determining current references ( $i_{d1}$ ,  $i_{q1}$ ,  $i_{d3}$ ,  $i_{q3}$ ) which guarantee the maximum torque and satisfy the constraints on voltage and current.

### 3.2 One phase in open-circuit fault

When one phase is open-circuited, it is necessary to have a continuous operation of the system with acceptable performances. It is assumed that the open-circuited fault happens in phase a and the proposed control strategies can be adapted for other open circuit faults. The current references in healthy mode are unsuitable for faulty cases so they need to be recalculated. In this case, new current references of healthy phases are denoted by  $i'_b$ ,  $i'_c$ ,  $i'_d$ ,  $i'_e$ ,  $i'_f$  and  $i'_g$ . There are different ways to determine the new current references.

$$H_1 = \begin{bmatrix} \cos(\theta - \frac{2\pi}{7}) - \cos(\theta - \frac{10\pi}{7}) & \cos(\theta - \frac{4\pi}{7}) - \cos(\theta - \frac{12\pi}{7}) & \cos(\theta - \frac{6\pi}{7}) - \cos(\theta - \frac{10\pi}{7}) & \cos(\theta - \frac{8\pi}{7}) - \cos(\theta - \frac{12\pi}{7}) \\ -\sin(\theta - \frac{2\pi}{7}) + \sin(\theta - \frac{10\pi}{7}) & -\sin(\theta - \frac{4\pi}{7}) + \sin(\theta - \frac{12\pi}{7}) & -\sin(\theta - \frac{6\pi}{7}) + \sin(\theta - \frac{10\pi}{7}) & -\sin(\theta - \frac{8\pi}{7}) + \sin(\theta - \frac{12\pi}{7}) \\ \cos(3\theta - \frac{6\pi}{7}) - \cos(3\theta - \frac{30\pi}{7}) & \cos(3\theta - \frac{12\pi}{7}) - \cos(3\theta - \frac{36\pi}{7}) & \cos(3\theta - \frac{18\pi}{7}) - \cos(3\theta - \frac{30\pi}{7}) & \cos(3\theta - \frac{24\pi}{7}) - \cos(3\theta - \frac{36\pi}{7}) \\ -\sin(3\theta - \frac{6\pi}{7}) + \sin(3\theta - \frac{30\pi}{7}) & -\sin(3\theta - \frac{12\pi}{7}) + \sin(3\theta - \frac{36\pi}{7}) & -\sin(3\theta - \frac{18\pi}{7}) + \sin(3\theta - \frac{30\pi}{7}) & -\sin(3\theta - \frac{24\pi}{7}) + \sin(3\theta - \frac{36\pi}{7}) \end{bmatrix} \quad (24)$$

$$H_2 = \begin{bmatrix} \cos(\theta - \frac{4\pi}{7}) - \cos(\theta - \frac{12\pi}{7}) & \cos(\theta - \frac{6\pi}{7}) - \cos(\theta - \frac{12\pi}{7}) & \cos(\theta - \frac{8\pi}{7}) - \cos(\theta - \frac{12\pi}{7}) & \cos(\theta - \frac{10\pi}{7}) - \cos(\theta - \frac{12\pi}{7}) \\ -\sin(\theta - \frac{4\pi}{7}) + \sin(\theta - \frac{12\pi}{7}) & -\sin(\theta - \frac{6\pi}{7}) + \sin(\theta - \frac{12\pi}{7}) & -\sin(\theta - \frac{8\pi}{7}) + \sin(\theta - \frac{12\pi}{7}) & -\sin(\theta - \frac{10\pi}{7}) + \sin(\theta - \frac{12\pi}{7}) \\ \cos(3\theta - \frac{12\pi}{7}) - \cos(3\theta - \frac{36\pi}{7}) & \cos(3\theta - \frac{18\pi}{7}) - \cos(3\theta - \frac{36\pi}{7}) & \cos(3\theta - \frac{24\pi}{7}) - \cos(3\theta - \frac{36\pi}{7}) & \cos(3\theta - \frac{30\pi}{7}) - \cos(3\theta - \frac{36\pi}{7}) \\ -\sin(3\theta - \frac{12\pi}{7}) + \sin(3\theta - \frac{36\pi}{7}) & -\sin(3\theta - \frac{18\pi}{7}) + \sin(3\theta - \frac{36\pi}{7}) & -\sin(3\theta - \frac{24\pi}{7}) + \sin(3\theta - \frac{36\pi}{7}) & -\sin(3\theta - \frac{30\pi}{7}) + \sin(3\theta - \frac{36\pi}{7}) \end{bmatrix} \quad (25)$$

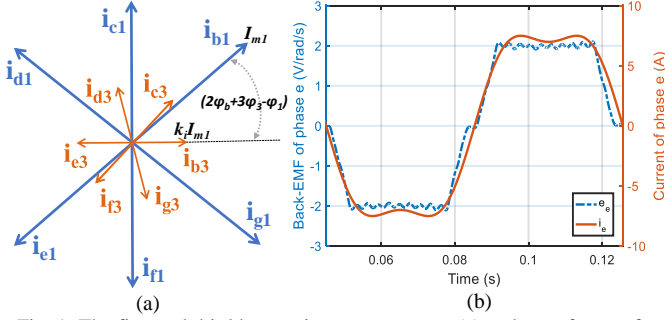


Fig. 1: The first and third harmonic current vectors (a) and waveforms of a current reference and experimental back-EMF in phase e (b) by method (IV).

Method	Imposed harmonics in current references	Frame
(I)	1 <sup>st</sup>	d-q
(II)	1 <sup>st</sup> and 3 <sup>rd</sup>	d-q
(III)	1 <sup>st</sup>	natural
(IV)	1 <sup>st</sup> and 3 <sup>rd</sup>	natural

Table 1: Control strategies when phase a is open-circuited.

In this section, four methods based on imposing the current references in d-q frames (methods (I-II) in Table 1) and in natural frame (methods (III-IV) in Table 1) are introduced. Their performances will be compared in the numerical result section.

### 3.2.1 Impose current references in d-q frames

Equations (7-10) describe relationships between currents in d-q frames and in natural frame.

$$i'_{d1} = \sqrt{\frac{2}{7}} \left\{ \begin{array}{l} i'_b \cos(\theta - \frac{2\pi}{7}) + i'_c \cos(\theta - \frac{4\pi}{7}) + i'_d \cos(\theta - \frac{6\pi}{7}) \\ + i'_e \cos(\theta - \frac{8\pi}{7}) + i'_f \cos(\theta - \frac{10\pi}{7}) + i'_g \cos(\theta - \frac{12\pi}{7}) \end{array} \right\} \quad (7)$$

$$i'_{q1} = \sqrt{\frac{2}{7}} \left\{ \begin{array}{l} -i'_b \sin(\theta - \frac{2\pi}{7}) - i'_c \sin(\theta - \frac{4\pi}{7}) - i'_d \sin(\theta - \frac{6\pi}{7}) \\ - i'_e \sin(\theta - \frac{8\pi}{7}) - i'_f \sin(\theta - \frac{10\pi}{7}) - i'_g \sin(\theta - \frac{12\pi}{7}) \end{array} \right\} \quad (8)$$

$$i'_{d3} = \sqrt{\frac{2}{7}} \left\{ \begin{array}{l} i'_b \cos(3(\theta - \frac{2\pi}{7})) + i'_c \cos(3(\theta - \frac{4\pi}{7})) \\ + i'_d \cos(3(\theta - \frac{6\pi}{7})) + i'_e \cos(3(\theta - \frac{8\pi}{7})) \\ + i'_f \cos(3(\theta - \frac{10\pi}{7})) + i'_g \cos(3(\theta - \frac{12\pi}{7})) \end{array} \right\} \quad (9)$$

$$i'_{q3} = \sqrt{\frac{2}{7}} \left\{ \begin{array}{l} -i'_b \sin(3(\theta - \frac{2\pi}{7})) - i'_c \sin(3(\theta - \frac{4\pi}{7})) \\ - i'_d \sin(3(\theta - \frac{6\pi}{7})) - i'_e \sin(3(\theta - \frac{8\pi}{7})) \\ - i'_f \sin(3(\theta - \frac{10\pi}{7})) - i'_g \sin(3(\theta - \frac{12\pi}{7})) \end{array} \right\} \quad (10)$$

Because of wye connected windings, new current references are required to respect Equation (11).

$$i'_b + i'_c + i'_d + i'_e + i'_f + i'_g = 0 \quad (11)$$

However, there are only five Equations (7-11) while the system has six unknown currents ( $i'_b, i'_c, i'_d, i'_e, i'_f, i'_g$ ). This leads to a lack of one equation to calculate the new current references.

The study proposes a new equation as presented in Equation (12) to find current solutions easily.

$$i'_b + i'_d + i'_f = 0 \quad (12)$$

Thus, new phase currents ( $i'_{d1}, i'_{q1}, i'_{d3}, i'_{q3}$ ) in Equation (13).

$$\vec{i}' = \sqrt{\frac{2}{7}} (H_1^{-1}) \vec{i}'_{dq} \quad (13)$$

where  $\vec{i}' = [i'_b \ i'_c \ i'_d \ i'_e]^T$  and  $\vec{i}'_{dq} = [i'_{d1} \ i'_{q1} \ i'_{d3} \ i'_{q3}]^T$ ;  $H_1$  is a 4 by 4 coefficient matrix as written in Equation (24) to find the current solution. From Equations (11-12), currents in phase f and phase g are determined as follows:

$$i'_f = -(i'_b + i'_d) \quad (14)$$

$$i'_g = -(i'_c + i'_e) \quad (15)$$

In Table 1, method (I) is when only the first harmonics are used,  $i'_{d3}$  and  $i'_{q3}$  must be nullified ( $i'_{d3} = i'_{q3} = 0$ ). In case both the first and third harmonics of currents are imposed to optimize the torque, we have method (II).

The optimization of torque for each value of the rotating speed must satisfy constrains on current and voltage in Equations (16-17).

$$[|i'_b|; |i'_c|; |i'_d|; |i'_e|; |i'_f|; |i'_g|] \leq I_{max} \quad (16)$$

$$[|v'_b|; |v'_c|; |v'_d|; |v'_e|; |v'_f|; |v'_g|] \leq V_{max} \quad (17)$$

### 3.2.2 Impose current references in natural frame

Another method for one open-circuited fault is proposed to improve the torque production. New current references in the natural frame are expressed in Equations (18-23). The first and third harmonic current vectors at initial point ( $\omega t = 0$ ) are shown in Fig. 1a.

$$i'_b = I_{m1} \sin(\omega t + \varphi_b + \varphi_1) + k_i I_{m1} \sin(3(\omega t + \varphi_b + \varphi_3)) \quad (18)$$

$$i'_c = I_{m1} \sin(\omega t + \varphi_c + \varphi_1) + k_i I_{m1} \sin(3(\omega t + \varphi_c + \varphi_3)) \quad (19)$$

$$i'_d = I_{m1} \sin(\omega t + \varphi_d + \varphi_1) + k_i I_{m1} \sin(3(\omega t + \varphi_d + \varphi_3)) \quad (20)$$

$$i'_e = -i'_b \quad (21)$$

$$i'_f = -i'_c \quad (22)$$

$$i'_g = -i'_d \quad (23)$$

$$H_3 = \begin{bmatrix} \cos(\theta - \frac{2\pi}{7}) - \cos(\theta - \frac{12\pi}{7}) & \cos(\theta - \frac{6\pi}{7}) - \cos(\theta - \frac{12\pi}{7}) & \cos(\theta - \frac{8\pi}{7}) - \cos(\theta - \frac{12\pi}{7}) & \cos(\theta - \frac{10\pi}{7}) - \cos(\theta - \frac{12\pi}{7}) \\ -\sin(\theta - \frac{2\pi}{7}) + \sin(\theta - \frac{12\pi}{7}) & -\sin(\theta - \frac{6\pi}{7}) + \sin(\theta - \frac{12\pi}{7}) & -\sin(\theta - \frac{8\pi}{7}) + \sin(\theta - \frac{12\pi}{7}) & -\sin(\theta - \frac{10\pi}{7}) + \sin(\theta - \frac{12\pi}{7}) \\ \cos(3\theta - \frac{6\pi}{7}) - \cos(3\theta - \frac{36\pi}{7}) & \cos(3\theta - \frac{18\pi}{7}) - \cos(3\theta - \frac{36\pi}{7}) & \cos(3\theta - \frac{24\pi}{7}) - \cos(3\theta - \frac{36\pi}{7}) & \cos(3\theta - \frac{30\pi}{7}) - \cos(3\theta - \frac{36\pi}{7}) \\ -\sin(3\theta - \frac{6\pi}{7}) + \sin(3\theta - \frac{36\pi}{7}) & -\sin(3\theta - \frac{18\pi}{7}) + \sin(3\theta - \frac{36\pi}{7}) & -\sin(3\theta - \frac{24\pi}{7}) + \sin(3\theta - \frac{36\pi}{7}) & -\sin(3\theta - \frac{30\pi}{7}) + \sin(3\theta - \frac{36\pi}{7}) \end{bmatrix} \quad (40)$$

$$H_4 = \begin{bmatrix} \cos(\theta - \frac{2\pi}{7}) - \cos(\theta - \frac{12\pi}{7}) & \cos(\theta - \frac{4\pi}{7}) - \cos(\theta - \frac{12\pi}{7}) & \cos(\theta - \frac{8\pi}{7}) - \cos(\theta - \frac{12\pi}{7}) & \cos(\theta - \frac{10\pi}{7}) - \cos(\theta - \frac{12\pi}{7}) \\ -\sin(\theta - \frac{2\pi}{7}) + \sin(\theta - \frac{12\pi}{7}) & -\sin(\theta - \frac{4\pi}{7}) + \sin(\theta - \frac{12\pi}{7}) & -\sin(\theta - \frac{8\pi}{7}) + \sin(\theta - \frac{12\pi}{7}) & -\sin(\theta - \frac{10\pi}{7}) + \sin(\theta - \frac{12\pi}{7}) \\ \cos(3\theta - \frac{6\pi}{7}) - \cos(3\theta - \frac{36\pi}{7}) & \cos(3\theta - \frac{12\pi}{7}) - \cos(3\theta - \frac{36\pi}{7}) & \cos(3\theta - \frac{24\pi}{7}) - \cos(3\theta - \frac{36\pi}{7}) & \cos(3\theta - \frac{30\pi}{7}) - \cos(3\theta - \frac{36\pi}{7}) \\ -\sin(3\theta - \frac{6\pi}{7}) + \sin(3\theta - \frac{36\pi}{7}) & -\sin(3\theta - \frac{12\pi}{7}) + \sin(3\theta - \frac{36\pi}{7}) & -\sin(3\theta - \frac{24\pi}{7}) + \sin(3\theta - \frac{36\pi}{7}) & -\sin(3\theta - \frac{30\pi}{7}) + \sin(3\theta - \frac{36\pi}{7}) \end{bmatrix} \quad (41)$$

where  $I_{m1}$  is the peak value of the first harmonic currents;  $k_i$  is the ratio between the third and first harmonics of the currents;  $\varphi_b$ ,  $\varphi_c$  and  $\varphi_d$  are constant initial phase angles of phase b, c and d respectively determined by the method in [9];  $\varphi_1$  and  $\varphi_3$  are adjustable angles of the first and third harmonics of currents;  $\omega$  is the electrical speed of the machine.

The proposed current references have the same amplitude with the objective to obtain equal copper losses in the healthy phases. The above references of currents also satisfy the assumption of the wye connection because the sum of all instantaneous currents is zero. If only the first harmonics of phase currents are used,  $k_i$  is set to be zero, we have method (III) in Table 1. Otherwise, method (IV) in Table 1 imposes both harmonics of currents, the waveform of each healthy phase current is like the corresponding experimental back-EMF as shown in Fig. 1b. This similarity allows the machine to produce the maximum torque. Magnitude ( $I_{m1}$ ), ratio ( $k_i$ ) and phase angles ( $\varphi_1, \varphi_3$ ) are estimated by `fmincon` in MATLAB. Then, these current references can be converted into d-q frames by using Concordia and Park transformations.

### 3.3 Two phases in open-circuit fault

#### 3.3.1 Two adjacent open-circuited phases

Phase a and b are assumed to be open-circuited. New current references ( $i_c'', i_d'', i_e'', i_f'', i_g''$ ) need to satisfy Equations (26-29).

$$i_{d1}'' = \sqrt{\frac{2}{7}} \left\{ \begin{array}{l} i_c'' \cos(\theta - \frac{4\pi}{7}) + i_d'' \cos(\theta - \frac{6\pi}{7}) \\ + i_e'' \cos(\theta - \frac{8\pi}{7}) + i_f'' \cos(\theta - \frac{10\pi}{7}) + i_g'' \cos(\theta - \frac{12\pi}{7}) \end{array} \right\} \quad (26)$$

$$i_{q1}'' = \sqrt{\frac{2}{7}} \left\{ \begin{array}{l} -i_c'' \sin(\theta - \frac{4\pi}{7}) - i_d'' \sin(\theta - \frac{6\pi}{7}) \\ - i_e'' \sin(\theta - \frac{8\pi}{7}) - i_f'' \sin(\theta - \frac{10\pi}{7}) - i_g'' \sin(\theta - \frac{12\pi}{7}) \end{array} \right\} \quad (27)$$

$$i_{d3}'' = \sqrt{\frac{2}{7}} \left\{ \begin{array}{l} i_c'' \cos(3(\theta - \frac{4\pi}{7})) + i_d'' \cos(3(\theta - \frac{6\pi}{7})) \\ + i_e'' \cos(3(\theta - \frac{8\pi}{7})) + i_f'' \cos(3(\theta - \frac{10\pi}{7})) \\ + i_g'' \cos(3(\theta - \frac{12\pi}{7})) \end{array} \right\} \quad (28)$$

$$i_{q3}'' = \sqrt{\frac{2}{7}} \left\{ \begin{array}{l} -i_c'' \sin(3(\theta - \frac{4\pi}{7})) - i_d'' \sin(3(\theta - \frac{6\pi}{7})) \\ - i_e'' \sin(3(\theta - \frac{8\pi}{7})) - i_f'' \sin(3(\theta - \frac{10\pi}{7})) \\ - i_g'' \sin(3(\theta - \frac{12\pi}{7})) \end{array} \right\} \quad (29)$$

As the machine is wye connected, the sum of healthy phase currents must be zero. There are 5 equations for 5 unknown currents, hence the solution is unique and determined by solving Equations (30-31).

$$\vec{i}'' = \sqrt{\frac{2}{7}} (H_2^{-1}) \vec{i}_{dq}'' \quad (30)$$

$$i_g'' = -(i_c'' + i_d'' + i_e'' + i_f'') \quad (31)$$

where  $\vec{i}'' = [i_c'' \ i_d'' \ i_e'' \ i_f'']^T$  and  $\vec{i}_{dq}'' = [i_{d1}'' \ i_{q1}'' \ i_{d3}'' \ i_{q3}'']^T$ ;  $H_2$  is a 4 by 4 coefficient matrix as written in Equation (25) to find the current solution.

Constraints on current and voltage are shown in Equations (32-33).

$$[|i_c''|; |i_d''|; |i_e''|; |i_f''|; |i_g''] \leq I_{max} \quad (32)$$

$$[|v_c''|; |v_d''|; |v_e''|; |v_f''|; |v_g'']] \leq V_{max} \quad (33)$$

#### 3.3.2 Two non-adjacent open-circuited phases

Due to the regular circular distribution of the phases, there are 2 cases of two non-adjacent opened phases in the seven-phase machine: phase a and c displaced by  $4\pi/7$ ; phase a and d displaced by  $6\pi/7$ . Constraints on current and voltage must be respected as in the previous case.

##### a) Phase a and c are open-circuited

When phase a and c are open-circuited, new current references are determined according to Equations (34-37) and the assumption about the wye connection.

$$i_{d1}'' = \sqrt{\frac{2}{7}} \left\{ \begin{array}{l} i_b'' \cos(\theta - \frac{2\pi}{7}) + i_d'' \cos(\theta - \frac{6\pi}{7}) + i_e'' \cos(\theta - \frac{8\pi}{7}) \\ + i_f'' \cos(\theta - \frac{10\pi}{7}) + i_g'' \cos(\theta - \frac{12\pi}{7}) \end{array} \right\} \quad (34)$$

$$i_{q1}'' = \sqrt{\frac{2}{7}} \left\{ \begin{array}{l} -i_b'' \sin(\theta - \frac{2\pi}{7}) - i_d'' \sin(\theta - \frac{6\pi}{7}) - i_e'' \sin(\theta - \frac{8\pi}{7}) \\ - i_f'' \sin(\theta - \frac{10\pi}{7}) - i_g'' \sin(\theta - \frac{12\pi}{7}) \end{array} \right\} \quad (35)$$

$$i_{d3}'' = \sqrt{\frac{2}{7}} \left\{ \begin{array}{l} i_b'' \cos(3(\theta - \frac{2\pi}{7})) + i_d'' \cos(3(\theta - \frac{6\pi}{7})) \\ + i_e'' \cos(3(\theta - \frac{8\pi}{7})) + i_f'' \cos(3(\theta - \frac{10\pi}{7})) \\ + i_g'' \cos(3(\theta - \frac{12\pi}{7})) \end{array} \right\} \quad (36)$$

$$i_{q3}'' = \sqrt{\frac{2}{7}} \left\{ \begin{array}{l} -i_b'' \sin(3(\theta - \frac{2\pi}{7})) - i_d'' \sin(3(\theta - \frac{6\pi}{7})) \\ - i_e'' \sin(3(\theta - \frac{8\pi}{7})) - i_f'' \sin(3(\theta - \frac{10\pi}{7})) \\ - i_g'' \sin(3(\theta - \frac{12\pi}{7})) \end{array} \right\} \quad (37)$$

Like the previous case, the new phase currents will be determined by solving Equations (38-39).

$$\vec{i}'' = \sqrt{\frac{2}{7}} (H_3^{-1}) \vec{i}_{dq}'' \quad (38)$$

$$i_g'' = -(i_b'' + i_d'' + i_e'' + i_f'') \quad (39)$$

where  $\vec{i}'' = [i_b'' \ i_d'' \ i_e'' \ i_f'']^T$  and  $\vec{i}_{dq}'' = [i_{d1}'' \ i_{q1}'' \ i_{d3}'' \ i_{q3}'']^T$ ;  $H_3$  is a 4 by 4 coefficient matrix in Equation (40) to find the current solution.

#### b) Phase a and d are open-circuited

In case phase a and d are open-circuited, new current references must satisfy Equations (42-45).

$$i_{d1}'' = \sqrt{\frac{2}{7}} \left\{ \begin{array}{l} i_b'' \cos(\theta - \frac{2\pi}{7}) + i_c'' \cos(\theta - \frac{4\pi}{7}) + i_e'' \cos(\theta - \frac{8\pi}{7}) \\ + i_f'' \cos(\theta - \frac{10\pi}{7}) + i_g'' \cos(\theta - \frac{12\pi}{7}) \end{array} \right\} \quad (42)$$

$$i_{q1}'' = \sqrt{\frac{2}{7}} \left\{ \begin{array}{l} -i_b'' \sin(\theta - \frac{2\pi}{7}) - i_c'' \sin(\theta - \frac{4\pi}{7}) - i_e'' \sin(\theta - \frac{8\pi}{7}) \\ - i_f'' \sin(\theta - \frac{10\pi}{7}) - i_g'' \sin(\theta - \frac{12\pi}{7}) \end{array} \right\} \quad (43)$$

$$i_{d3}'' = \sqrt{\frac{2}{7}} \left\{ \begin{array}{l} i_b'' \cos(3(\theta - \frac{2\pi}{7})) + i_c'' \cos(3(\theta - \frac{4\pi}{7})) \\ + i_e'' \cos(3(\theta - \frac{8\pi}{7})) + i_f'' \cos(3(\theta - \frac{10\pi}{7})) \\ + i_g'' \cos(3(\theta - \frac{12\pi}{7})) \end{array} \right\} \quad (44)$$

$$i_{q3}'' = \sqrt{\frac{2}{7}} \left\{ \begin{array}{l} -i_b'' \sin(3(\theta - \frac{2\pi}{7})) - i_c'' \sin(3(\theta - \frac{4\pi}{7})) \\ - i_e'' \sin(3(\theta - \frac{8\pi}{7})) - i_f'' \sin(3(\theta - \frac{10\pi}{7})) \\ - i_g'' \sin(3(\theta - \frac{12\pi}{7})) \end{array} \right\} \quad (45)$$

The new phase currents are obtained by solving Equations (46-47).

$$\vec{i}'' = \sqrt{\frac{2}{7}} (H_4^{-1}) \vec{i}_{dq}'' \quad (46)$$

$$i_g'' = -(i_b'' + i_c'' + i_e'' + i_f'') \quad (47)$$

where  $\vec{i}'' = [i_b'' \ i_c'' \ i_e'' \ i_f'']^T$  and  $\vec{i}_{dq}'' = [i_{d1}'' \ i_{q1}'' \ i_{d3}'' \ i_{q3}'']^T$ ;  $H_4$  is a 4 by 4 coefficient matrix as written in Equation (41) to find the current solution.

## 4 Numerical Results

The torque optimizations under constraints are implemented by using `fmincon` function in MATLAB. Parameters of the converter and seven-phase BLDC machine are shown in Table 2. In this machine, the amplitude of the third harmonics of back-EMFs equals about 19% of the first harmonics. The converter is supplied by a DC bus voltage of 200V with the maximum peak current of 7.5A. Thus, the constraints are carried out with  $V_{max}=100$  V and  $I_{max}=7.5$  A. In Fig. 2, a control scheme of the drive system is presented. In optimization block, `fmincon` estimates variables such as current references in d-q frames ( $i_{d1}''$ ,  $i_{q1}''$ ,  $i_{d3}''$ ,  $i_{q3}''$ ) or parameters of currents in natural frame ( $I_{m1}$ ,  $k_i$ ,  $\varphi_1$ ,  $\varphi_3$ ) to maximize the torque and respect the constraints. Then, the current references at each rotating speed in a certain fault obtained from the above optimization step are stored in a look-up table for current impositions. In Figs. 3-4, the average torques and torque ripples of the system in single open-phase fault (phase a) by 4 methods (in Table 1) compared to the healthy mode are presented. In Fig. 3, the optimal torque in healthy mode is 74.5 Nm. When phase a is opened, method (I) produces an average torque equal to about 50% of the healthy mode while that of method (II) is slightly higher with 58% due to the presence of the third harmonics of current

references. Method (III) imposing only the first harmonics of currents in natural frame gives an average torque equal to 68% of the healthy torque. By applying both harmonics of currents in natural frame, the torque by method (IV) is highest and equal to 80% of the healthy mode. In Fig. 4, torque ripples of (I) and (II) are zero like the healthy mode since constant currents in d-q frames are imposed. Besides, method (III) has 13% torque ripples while that of method (IV) is only 7% and remains unchanged in the whole range of rotating speed including the flux-weakening region. In Fig. 5a, average torques in the case of double open-phase faults (a-b, a-c and a-d) equal approximately 42%, 24% and 34% of the healthy one, respectively. Although only two phases over seven phases are open-circuited, the torques decrease more than 50% due to the constraints on current and voltage. Power-speed characteristics in all operation modes are illustrated in Fig. 5b. Fig. 6 shows that phase currents and voltages respect their constraints in all cases of the system when their values do not exceed  $I_{max}=7.5$  A and  $V_{max}=100$  V. Phase currents with peak value bounded by  $I_{max}$  at 21rad/s when phase a is opened and when both phase a and b are opened are shown in Figs. 7a and 7b respectively.

Parameter	Value
Stator resistance ( $\Omega$ )	1.4
Phase inductance (mH)	10.1
Mutual inductance $M_1$ (mH)	3.1
Mutual inductance $M_2$ (mH)	-1.05
Mutual inductance $M_3$ (mH)	-5.3
Number of pole pairs p	3
Speed-normalized amplitude of 1 <sup>st</sup> harmonic EMF (V/rad/s)	2.38
Speed-normalized amplitude of 3 <sup>rd</sup> harmonic EMF (V/rad/s)	0.45
DC-bus voltage (V)	200
Maximum peak current (A)	7.5

Table 2: Electrical parameters of the converter and machine.

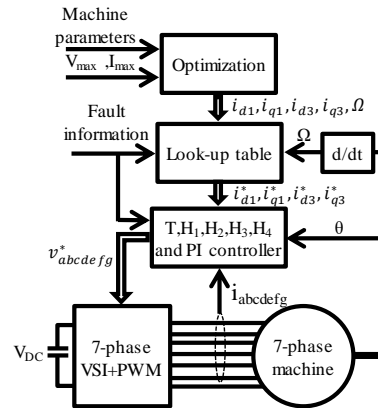


Fig. 2: Control scheme of the drive system.

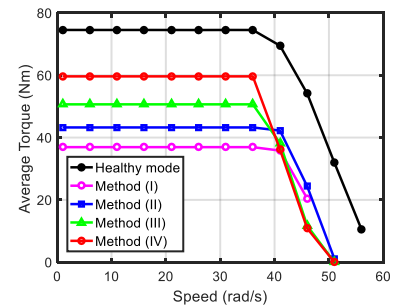


Fig. 3: Average torques by 4 methods when only phase a is open-circuited.



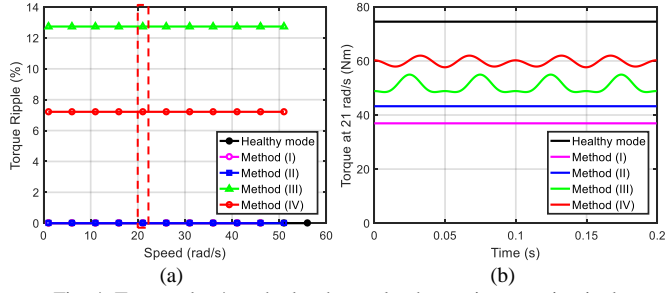


Fig. 4: Torques by 4 methods when only phase a is open-circuited: (a) Torque ripples vs speed; (b) Torque vs time at 21 rad/s.

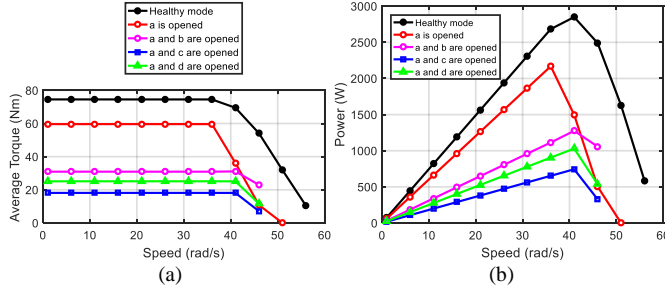


Fig. 5: Average torque (a) and power (b) in terms of speed in all operation modes in which method (IV) is used when only phase a is open-circuited.

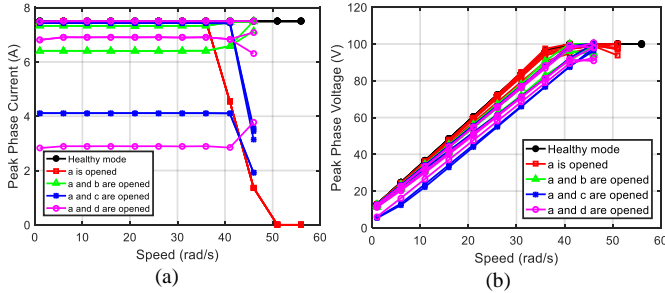


Fig. 6: Constrains on current and voltage in all operation modes where method (IV) is used when only phase a is open-circuited: (a) Peak phase currents vs speed; (b) Peak phase voltages vs speed.

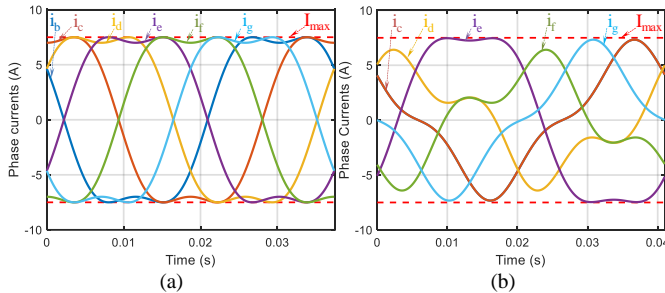


Fig. 7: Current references at 21 rad/s: (a) Phase a is open-circuited (using method (IV)); (b) Phase a and b are open-circuited.

## 5 Conclusions

The paper has proposed control strategies for a seven-phase BLDC machine with trapezoidal back-EMFs. The methods enable the system to work properly with optimal torques in healthy or faulty modes, including the flux-weakening operation. The constraints on current and voltage defined from parameters of the machine-converter system are respected. In faulty cases, by imposing constant currents in d-q frames ( $i'_{d1}$ ,  $i'_{q1}$ ,  $i'_{d3}$  and  $i'_{q3}$  are constants), it is simple to control the machine. However, the fifth harmonic components ( $i'_{d5}$  and

$i'_{q5}$ ) are inconstant and must be tracked properly. Imposing the first and third harmonic of currents in natural frame cannot ensure a zero-torque ripple, unless a compensation in d-q frames by using inverse components is applied. Analytical formulations have been presented for all operation modes in this study. The system is simulated by MATLAB to verify the usefulness of the proposed control strategies. In future, these methods would be validated by experimental tests.

## References

- [1] F. Barrero and M. J. Duran, "Recent Advances in the Design, Modeling, and Control of Multiphase Machines Part I," *IEEE Transactions on Industrial Electronics*, vol. 63, pp. 449-458, 2016.
- [2] M. J. Duran and F. Barrero, "Recent Advances in the Design, Modeling, and Control of Multiphase Machines Part II," *IEEE Transactions on Industrial Electronics*, vol. 63, pp. 459-468, 2016.
- [3] F. Locment, E. Semail, and X. Kestelyn, "Vectorial Approach-Based Control of a Seven-Phase Axial Flux Machine Designed for Fault Operation," *IEEE Transactions on Industrial Electronics*, vol. 55, pp. 3682-3691, 2008.
- [4] S. Dwari and L. Parsa, "Fault-Tolerant Control of Five-Phase Permanent-Magnet Motors With Trapezoidal Back EMF," *IEEE Transactions on Industrial Electronics*, vol. 58, pp. 476-485, 2011.
- [5] A. Mohammadpour and L. Parsa, "A Unified Fault-Tolerant Current Control Approach for Five-Phase PM Motors With Trapezoidal Back EMF Under Different Stator Winding Connections," *IEEE Transactions on Power Electronics*, vol. 28, pp. 3517-3527, 2013.
- [6] S. Dwari and L. Parsa, "Open-circuit fault tolerant control of five-phase permanent magnet motors with third-harmonic back-EMF," in *2008 34th Annual Conference of IEEE Industrial Electronics*, 2008, pp. 3114-3119.
- [7] Z. Sun, J. Wang, G. W. Jewell, and D. Howe, "Enhanced Optimal Torque Control of Fault-Tolerant PM Machine Under Flux-Weakening Operation," *IEEE Transactions on Industrial Electronics*, vol. 57, pp. 344-353, 2010.
- [8] O. Fall, N. K. Nguyen, J. F. Charpentier, P. Letellier, E. Semail, and X. Kestelyn, "Variable speed control of a 5-phase permanent magnet synchronous generator including voltage and current limits in healthy and open-circuited modes," *Electric Power Systems Research*, vol. 140, pp. 507-516, 11/2016.
- [9] F. Jen-Ren and T. A. Lipo, "Disturbance-free operation of a multiphase current-regulated motor drive with an opened phase," *IEEE Transactions on Industry Applications*, vol. 30, pp. 1267-1274, 1994.
- [10] H. Zhou, W. Zhao, G. Liu, R. Cheng, and Y. Xie, "Remedial Field-Oriented Control of Five-Phase Fault-Tolerant Permanent-Magnet Motor by Using Reduced-Order Transformation Matrices," *IEEE Transactions on Industrial Electronics*, vol. 64, pp. 169-178, 2017.
- [11] B. Tian, Q. T. An, J. D. Duan, D. Y. Sun, L. Sun, and D. Semenov, "Decoupled Modeling and Nonlinear Speed Control for Five-Phase PM Motor Under Single-Phase Open Fault," *IEEE Transactions on Power Electronics*, vol. 32, pp. 5473-5486, 2017.
- [12] G. Liu, Z. Lin, W. Zhao, Q. Chen, and G. Xu, "Third Harmonic Current Injection in Fault-Tolerant Five-Phase Permanent-Magnet Motor Drive," *IEEE Transactions on Power Electronics*, vol. PP, pp. 1-10, 2017.
- [13] F. Locment, E. Semail, and X. Kestelyn, "Optimum use of DC bus by fitting the back-electromotive force of a 7-phase permanent magnet synchronous machine," in *2005 European Conference on Power Electronics and Applications*, 2005, pp. 1-9.
- [14] F. Locment, E. Semail, and F. Piriou, "Design and study of a multiphase axial-flux machine," *IEEE Transactions on Magnetics*, vol. 42, pp. 1427-1430, 2006.
- [15] E. Semail, A. Bouscayrol, and J. P. Hautier, "Vectorial formalism for analysis and design of polyphase synchronous machines," *Eur. Phys. J. AP*, vol. 22, pp. 207-220, 6/2003.
- [16] E. Semail, X. Kestelyn, and A. Bouscayrol, "Right harmonic spectrum for the back-electromotive force of an n-phase synchronous motor," in *Conference Record of the 2004 IEEE Industry Applications Conference, 2004. 39th IAS Annual Meeting*, 2004, pp. 71-78.